COMPUTATIONS OF DOWNWARD RADIATION FLUX BASED UPON A RANDOM SAMPLE OF RADIOSONDE OBSERVATIONS, AND CORRELATION OF THE RESULTS WITH CORRESPONDING SIMULATED NIMBUS II SATELLITE AIR MASS PROPERTIES

JESUS BONIFACIO TUPAZ

COMPUTATIONS OF DOWNWARD RADIATION FLUX BASED UPON A RANDOM SAMPLE OF RADIOSONDE OBSERVATIONS, AND CORRELATION OF THE RESULTS WITH CORRESPONDING SIMULATED NIMBUS II SATELLITE AIR MASS PROPERTIES

by

Jesus Bonifacio Tupaz
Lieutenant, United States Navy
B.S., Naval Academy, 1960

Submitted in partial fulfillment of the
requirements for the degree of

MASTER OF SCIENCE IN METEOROLOGY

from the

NAVAL POSTGRADUATE SCHOOL
June 1967

ABSTRACT

Relying heavily on the Elsasser and Culbertson (1960) computational system, computations of terrestrial radiation incident at a black body interface have been programmed for an arbitrary atmospheric sounding. The program has been applied to a random sampling of 62 radiosondes from the "Wark-sounding-catalog."

Since Wark et al. (1966) have kindly made available simulated Nimbus II channel 2 and channel 4 specific intensities for these same atmospheres, a multivariate regression was derived relating downward flux computations to Nimbus II channel 2 and channel 4 readouts as well as to two other gross air parameters: (a) total reduced water vapor depth, and (b) interface pressure. All four independent variables gave high statistical significance, with channel 4 filtered flux accounting for the major portion of the "explained variance" of the dependent variable. Total ozone was also tested but yielded no statistical significance on the regression.

TABLE OF CONTENTS

LIST OF ILLUSTRATIONS

LIST OF TABLES

LIST OF SYMBOLS

Symbol	Meaning
A	constant in the 5 predictor regression plane
α^*	probability level of the multiple regression
A'	constant in the 4 predictor regression plane
α	critical probability level for the single predictor
B	black body radiation flux
f	subscript depicting the last interval in the sounding
F-statistic	computed F value
F'-critical value	tabulated F value
F_d	downward infrared flux of radiation
F_{wv}	downward infrared flux of radiation due to water vapor
F_{CO_2}	downward infrared flux of radiation due to CO_2
F_{O3}	downward infrared flux of radiation due to ozone
F'_d	estimated downward infrared flux of radiation by a regression equation
$\Delta F(u^*,\mathcal{U}^*)$	H_2O-CO_2 flux of radiation overlap
$\Delta F(u^*, U^*)$	H_2O-O_3 flux of radiation overlap
I	specific intensity of radiant energy
K	last interval in the sounding in a summation
k	number of predictors in a regression analysis
L_ν	general absorption coefficient, after Elsasser et al.
m	sequential order of the predictors from 1 through k

ν	wavenumber of downward infrared radiation flux in cm^{-1}
q	mixing ratio of water vapor
Q	mixing ratio of ozone
p	pressure
R	R value as obtained from Elsasser's Radiation Charts
R_k	multiple correlation coefficient
R_k^2	coefficient of determination
$\hat{R}_k$	effective multiple correlation coefficient
$\hat{R}_k^2$	effective coefficient of determination
σT_B^4	equivalent black body radiation flux from the interface
T	temperature
T_B	equivalent black body temperature
F_4	filtered channel 4 upward radiation flux
θ	zenith angle of specific intensity of radiant energy
τ_F	transmissivity of radiant energy
u	optical path of water vapor
u*	reduced optical path of water vapor
U	optical path of ozone
U*	reduced optical path of ozone
$\mathcal{U}$	optical path of carbon dioxide
$\mathcal{U}^*$	reduced optical path of carbon dioxide
$X_{i+1/2}$	mean value of parameter (X) between intervals i and i+1

$\Delta_{i+1/2}X$	difference value between X_i and X_{i+1}
y_i	RADFLUX computation of downward flux
y_i'	estimated F_d
$\bar{y}$	Mean value of observed F_d sample
Y	dependent variable in the 5 predictor regression
Y'	dependent variable in the 4 predictor regression
z	independent variables in the regressions

ACKNOWLEDGEMENTS

The advice and encouragement of Professor Frank L. Martin of the United States Naval Postgraduate School are gratefully acknowledged. Also, much appreciation is extended to Miss Sharon Raney of the United States Naval Postgraduate School Computer Facility for her professional help in the early stages of the computer programming.

1. Introduction

A knowledge of downward infrared radiation flux is required in order to understand properly the heat partitioning in the earth-atmosphere and sun system. The atmosphere is much more transparent to short-wave than to long-wave radiation. This is depicted by the absorption spectra for the atmospheric gases on p. 153 of Fleagle and Businger [6]. From these spectra, one can see that there is strong absorption in the infrared by water vapor, carbon dioxide and to a lesser degree by ozone. It is the goal of this paper to develop a computer program that is readily adaptable to computation of downward radiation flux from soundings using input sounding data from each of these three atmospheric constituents. As a by-product, the secondary goal is to relate empirically the results to a regression equation of selected satellite air mass properties.

Wark et al. [16] studied intensively the problem of upward flux and consequently compiled 106 randomly distributed radiosonde observations from the I.G.Y. files in what is hereby termed the "Wark-catalog." This composite set of soundings cover a wide range of radiative conditions. Moreover, simulated Nimbus II data was kindly provided by J.H. Lienesch of the National Satellite Center for the same 106 soundings. Downward infrared flux measurements may be made by the Kuhn-Suomi radiometer but these give only limited areal coverage compared to the MRR data from satellites; thus, it was decided to compute downward flux in a manner similar (not identical) to that employed by Wark et al. in his 1962 study, and to perform a multiple linear regression analysis with certain simulated Nimbus II channel-readout values as input variables. The computation of downward infrared flux is made

applicable to the top of the undercast cloud or to the ground level, but the computer programming is left flexible so as to apply to downward flux at an arbitrary number of sounding levels above the interface.

2. Nature of the Data

The 106 radiosonde observations in the Wark-Catalog are given as profile listings of pressure (mb), temperature (°K), mixing ratio of water vapor (g/kg), and mixing ratio of ozone (cm NTP per mb). Each sounding or case atmosphere is identified by a number, the name of the radiosonde station, and the date and time of the sounding. The sky conditions is indicated by "clear" or by the height (in mb) of the top of the undercast cloud. Temperatures and pressures are given at approximately 25 $\pm$ 5 selected levels as well as at the interface. The interface is defined for this study as being the earth's surface for clear cases or the top surface of the undercast for cloudy cases. Total (corrected) water vapor and ozone masses are also given in this Wark-catalog. The models developed by the Meterorological Satellite Laboratory were taken from radiosonde data over all latitudes and seasons. All the soundings were from the I.G.Y record-file and went to at least 25 mb. Above this level, temperatures were extrapolated parallel to the appropriate Supplementary Standard atmosphere to the pressure of 0.1 mb. Furthermore, stratospheric humidity was extrapolated to conform in general to the Supplementary Standard distribution for the particular air mass at the station (standard cP, standard mT air masses, etc.). The 62 cases selected are composed of 47 undercast cases at various altitudes and 15 clear cases, the latter being randomly selected from the Wark-catalog.

Nimbus II satellite data is used to compute filtered channel 4 upward radiation flux and the interface Black Body radiation flux for each of the 62 selected atmospheres. The Nimbus II data lists total and filtered channel 4 (5_μ to 30_μ) infrared specific intensities for five zenith angles (theta), that is, θ = 0°, 20°, 45°, 60°, and 78.5°. The specific intensities for θ = 90° are obtained by a Lagrangian form of extrapolation which is explained below in connection with equations (19) and (20). The radiation intensities of the 62 cases are listed in ergs/(cm^2sec stdn) and are converted to watts/(m^2 stdn) in this paper. It should be noted that the characteristics of the satellite infrared sensing-filter system must be eliminated so that the results do not depend upon this optical system to any appreciable degree. The National Satellite Laboratory minimized the channel 2 and channel 4 sensor-filter effects on the Nimbus II data by normalizing the filter-sensor response functions for the various IR wave channels, hence, the resulting response was the "best possible" estimate of the thermal flux (5-30μ) for the channel 4 radiometer, and of the black body flux (10-11μ) or its equivalent black body temperature for the channel 2 radiometer. Also, the sounding data lists temperature at the interface of each of the case atmospheres, which Keith [9] found to be very accurately described by the Nimbus II channel 2 readout.

3. Computation of Downward Flux of Radiation

Downward infrared flux of radiation arriving at the interface is quantitatively computed for each of the 62 selected atmospheres from the Wark-catalog by the Elsasser computational system. The downward flux computation is divided into five parts.

$$F_d = F_{wv} + F_{CO_2} + F_{O_3} - \Delta F(u^*, \mathcal{U}^*) - \Delta F(u^*, U^*) \quad (1)$$

The last two terms of equation (1) represent the "so called overlap of flux" and, hence, are subtracted from the first three terms of equation (1) which represents the downward infrared flux not corrected in any way from the manner described by Elsasser and Culbertson [5] (henceforth denoted by EC for abreviation). The computation of the terms of equation (1) is explained below in connection with equations (6) through (11).

In actuality, an energy-sharing process occurs in the 15μ and 9.6μ bands which correspond to the CO_2-H_2O and O_3-H_2O overlap fluxes, respectively, thus, accounting for the ΔF-terms. For example, according to Hanel, Bandeen, and Conrath [7], ozone should be considered the primary radiator in the 9.6μ band, hence, water vapor is the weak secondary absorber-radiator resulting in the correction due to the shared radiation, $\Delta F(u^*, U^*)$.

It is necessary to know the layer values of reduced optical path for water vapor, ozone, and carbon dioxide in the computation of radiative fluxes by each of the three constituents. The reduced optical path du* of an absorber has been taken from EC, and its relation to the true optical path is given by

$$du^* = \frac{P}{P_o}\left(\frac{T_o}{T}\right)^{\frac{1}{2}} du \quad (2)$$

According to EC [5], the dependence on temperature is slight and, hence, is excluded in this study. The finite difference relations for the resulting reduced optical paths of the three main constituents are given by

$$u^* = \sum_{i=1}^{K} \Delta_i u^*_i = \sum_{i=1}^{K} (q_{i+\frac{1}{2}})(p_{i+\frac{1}{2}})(\Delta_{i+\frac{1}{2}} p) \text{ X } 1.00705 \text{ X } 10^{-6} (g/cm^2) \quad (3)$$

$$U^* = \sum_{i=1}^{K} \Delta_i U^* = \sum_{i=1}^{K} (Q_{i+\frac{1}{2}}) \, (\Delta_{i+\frac{1}{2}} p) \times 10^{-5} \quad \text{(cm NTP)} \tag{4}$$

$$\mathcal{U}^* = \sum_{i=1}^{K} \Delta_i \mathcal{U}^* = \sum_{i=1}^{K} (p_{i+\frac{1}{2}}) \, (\Delta_{i+\frac{1}{2}} p) \times 2.4469 \times 10^{-4} \quad \text{(cm NTP)} \tag{5}$$

Basically, the EC computational technique for the determination of downward infrared radiation flux is realized by the integration of the area under the curve as shown in Fig. 1 with the use of Elsasser-Culbertson [5] flux tables of R(u*,T) which have been incorporated in the author's computer program RADFLUX found in Appendix I-A. In essence, one enters the EC tables with logarithmic values of the constituent optical paths and their corresponding temperatures, and obtains the respective "R" values which are explained below in connection with equations (6) through (11). These "R" values are then integrated over the entire temperature range of the sounding resulting in the flux of radiant energy due to the particular constituent. There are various forms that can be used to determine the energy integral but Elsasser et al. [5] and Yamamoto [17] used temperature instead of optical path (u) as the independent variable.

The "R" term has been taken from EC and is given by

$$R(u^*,T) = \int_{\nu_o}^{\nu_f} \frac{dB_\nu}{dT} (1-\tau_F(u^*) d\nu \, , \tag{6}$$

hence, one can readily see from equation (6) that infrared flux can be realized by an integration scheme of the R(u*,T) term over the temperature range. For example, downward infrared radiation flux for water vapor and its corresponding finite difference form are given by

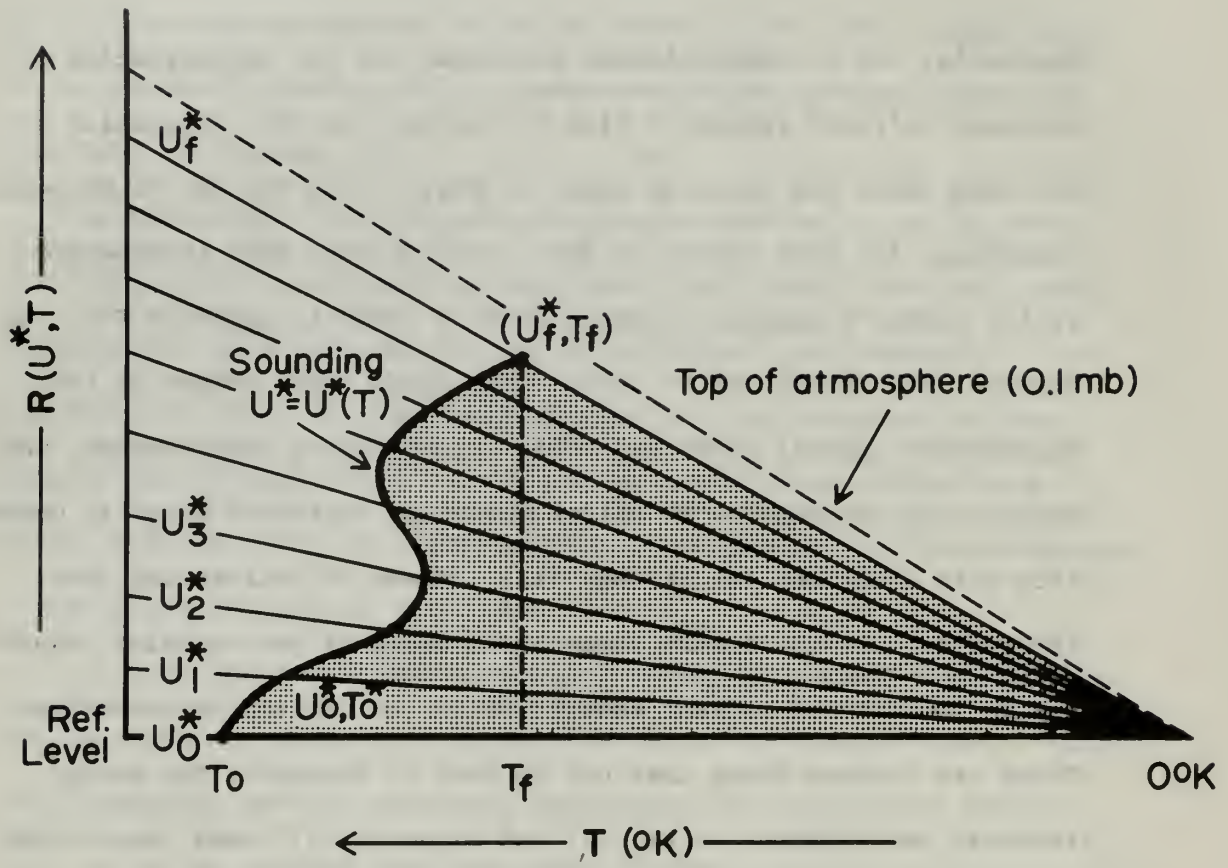

Fig. 1. Schematic form of the distribution of $R(U^*,T)$ from tables in Elsasser and Culbertson [5] as applied to a typical sounding representative of the U-T distribution for any of the three atmospheric constituents. The area bounded by the sounding and the isopleths $U^* = 0$ and $U^* = U_f$ is the downward flux uncorrected for possible overlap.

$$F_{wv} = \int_{o}^{T_f} R(u_f^*, T)dT + \int_{T_f}^{T_o} R[u^*(T), T]\, dT \qquad (7)$$

$$F_{wv} = \sum_{i=1}^{i=i_f} R_{i+\frac{1}{2}}(u^*_{i+\frac{1}{2}}, T_{i+\frac{1}{2}})\ (T_i - T_{i-1}) + \sum_{i=i_f}^{i=80^oC} R_{i+\frac{1}{2}}(u^*_f, T_i)(T_{i+1} - \hat{T}) + \int_{-80^oC}^{-273^oC} R(u_f^*, T)dT \qquad (8)$$

For water vapor, the range of wave number (ν_o, ν_f) is listed, by 40 cm^{-1} intervals, from 20 to 2600 cm^{-1}, which is regarded as spanning the effective infrared range of the terrestrial radiation spectrum. The finite difference approximation for the $R_{i+\frac{1}{2}}$ in equation (8) assumes the form given by

$$R_{i+\frac{1}{2}} = [R_i(u_i^*, T_i) + R_{i+1}(u_{i+1}^*, T_{i+1})]\ /2 \qquad (9)$$

and the last term of equation (8) is obtained from Table 20 of EC. A similar formulation for F_{CO_2} and F_{O_3} is realized by the use of Tables 11 and 13, respectively, in EC; however, R_{CO_2} and R_{O_3} values are restricted to the frequency ranges of 540-820 cm^{-1} and 970-1130 cm^{-1}, respectively.

The last two terms of equation (1), the H_2O-CO_2 and H_2O-O_3 overlap flux terms, are defined by the following expressions

$$\Delta F(u^*, \mathcal{U}^*) = \int_{o}^{T_f} \bar{\tau}_F(u^*_f) R_{CO_2}(\mathcal{U}^*_f, T)dT + \int_{T_f}^{T_o} \bar{\tau}_F(u^*) R_{CO_2}(\mathcal{U}^*, T)dT \qquad (10)$$

$$\Delta F(u^*, U^*) = \int_{o}^{T_f} \bar{\tau}_F(u^*_f) R_{O_3}(U^*_f, T)dT + \int_{T_f}^{T_o} \bar{\tau}_F(u^*) R_{O_3}(U^*, T)dT \qquad (11)$$

Moreover, values of $\bar{\tau}_F(u^*)$ in the H_2O-CO_2 overlap was determined by Martin [10] according to

$$\bar{\tau}_F(u^*) = \frac{\sum_{\nu_o}^{\nu_f} \tau_{F\nu} B_{\nu T} \Delta\nu}{\sum_{\nu_o}^{\nu_f} B_{\nu T} \Delta\nu} = \frac{\sum_{\nu_o}^{\nu_f} \left[\left(1 - \frac{2}{\sqrt{\pi}} \int_{o}^{x = \sqrt{L_\nu u^*}} e^{-t^2}\, dt \right) B_{\nu T}\ \Delta\nu \right]}{\sum_{\nu_o}^{\nu_f} B_{\nu T}\ \Delta\nu} \qquad (12)$$

where L_ν is the generalized absorption coefficient listed by 40 cm^{-1} intevals and $B_{\nu T}$ is the Planck specific black body flux for a given temperature. The results of this computation are shown in Table 1. The H_2O-CO_2 overlap flux occurs in the 540-820 cm^{-1} range, hence the water vapor $\overline{\tau}_F(u)$ within this range was obtained by performing the summation indicated by equation (12) using both $\tau_{F\nu}$, and $B_{\nu T}$ at 20°C, and at 40 cm^{-1} intervals. L_ν values were taken from Table 10 in EC. According to EC, 20°C is a representative base temperature for $\tau_{F\nu}$ observations since the H_2O-CO_2 overlap is in practice most important in the lower layers of the atmosphere. In contrast, Wark et al. [16] used Yamamoto's [17] $\tau_{F\nu o}$ values which were based upon theoretical transition probabilities; however, Palmer's [14] laboratory measurements made at 300°K seem to give good agreement with Yamamoto's values for 25 cm^{-1} intervals. After some additional smoothing, it was noted that the quoted L_ν values over 40 cm^{-1} intervals in Table 10 of EC corresponded closely to Yamamoto's quoted values of "$\ell_\nu/2$" because of the slightly wider interval used in EC.

Furthermore, $\overline{\overline{\tau}}_F(u^*)$ in the H_2O-O_3 overlap is given by

$$\overline{\overline{\tau}}_F(u^*) = \exp[-0.1167\ u^*] \qquad (13)$$

Equation (13) uses the continuum (970-1130 cm^{-1}) absorption coefficient of water vapor proposed by Hanel et al. [7]. In both the H_2O-CO_2 and H_2O-O_3 overlap regimes, the water-vapor sharing path has been increased by the factor 5/3 in order to transform beam transmissivity to flux transmissivity.

The results of the foregoing Elsasser computational scheme using the author's computer program RADFLUX on the 62 selected case atmospheres from the Wark-catalog are shown in Table 2 along

Table 1. Water vapor flux transmissivities in the H_2O-CO_2 overlap regime (540-820 cm^{-1}).

log u*	$\overline{\tau}_F(u^*)$	log u*	$\overline{\overline{\tau}}_F(u^*)$
-6.0	0.9999997150	-2.7	0.9994259
-5.7	0.9999994259	-2.3	0.998527
-5.3	0.999998527	-2.0	0.997150
-5.0	0.999997150	-1.7	0.994259
-4.7	0.999994259	-1.3	0.985665
-4.3	0.99998527	-.10	0.97128
-4.0	0.99997150	-0.7	0.94431
-3.7	0.99994259	-0.3	0.86680
-3.3	0.9998527	0	0.77328
-3.0	0.9997150	+0.3	0.67567
		+0.7	0.54833

with their corresponding case-number identifiers from this catalog. The table lists uncorrected fluxes for water vapor, ozone, and carbon dioxide together with the CO_2 and ozone overlaps. The CO_2 and ozone overlaps are equally partitioned arbitrarily between CO_2 and water vapor, and ozone and water vapor, respectively. As a result, half of the overlapped flux is restored to CO_2 and ozone, that is, the partitioned overlap fluxes are subtracted from their respective uncorrected constituent fluxes as shown below in connection with equations (14) through (16), thus, realizing corrected constituent fluxes.

$$F_{wv}(CORR) = F_{wv} - \Delta F(u^*,U^*)/2 - \Delta F(u^*,\mathcal{U}^*)/2 \quad (14)$$

$$F_{CO2}(CORR) = F_{CO_2} - \Delta F(u^*,\mathcal{U}^*)/2 \quad (15)$$

$$F_{O3}(CORR) = F_{O_3} - \Delta F(u^*,U^*)/2 \quad (16)$$

It should be noted that all the fluxes shown in Table 2 are in watts/m^2 and that the mean of each overlap and constituent flux as well as the average percent contribution of the corrected constituent flux on the total downward flux are given at the bottom of the table.

CASE	H2O-CO2 OVERLAP	H2O-O3 OVERLAP	UNCORRECTED WV FLUX	CORRECTED WV FLUX	UNCORRECTED O3 FLUX	CORRECTED O3 FLUX	UNCORRECTED CO2 FLUX	CORRECTED CO2 FLUX	TOTAL DOWNWARD FLUX
2	51.423	3.066	255.898	228.653	10.874	9.341	73.431	47.719	285.713
3	47.597	4.138	246.671	220.804	11.410	9.341	71.421	47.622	277.767
4	53.563	4.801	168.837	139.655	9.537	7.136	56.286	29.504	176.296
7	33.378	1.395	155.552	138.316	8.094	7.397	56.826	40.287	185.999
8	38.327	3.652	123.258	102.269	7.774	5.948	48.550	29.386	137.602
10	57.929	5.143	263.871	232.335	13.398	10.826	69.619	40.655	283.815
12	43.063	3.861	190.504	167.042	11.503	9.573	62.955	41.423	218.038
13	50.274	5.956	158.831	130.716	10.081	7.103	54.728	29.591	167.410
20	54.531	7.672	189.774	158.672	11.994	8.158	61.467	34.202	201.032
23	45.347	5.519	136.574	111.142	9.247	6.487	51.151	28.478	146.107
27	34.243	4.074	131.287	112.229	9.325	7.289	52.046	35.025	154.542
31	15.708	1.294	71.554	63.053	6.281	5.634	32.212	24.358	93.046
50	40.182	3.846	125.149	103.135	9.831	7.908	48.695	28.604	139.647
51	37.816	3.922	98.496	77.627	9.271	7.310	45.701	26.793	111.730
52	32.215	4.797	76.868	58.362	7.832	5.434	31.682	15.574	79.370
53	45.779	6.530	128.799	102.644	9.811	6.546	51.199	28.315	137.500
54	32.854	2.226	106.971	89.430	7.264	6.150	42.632	26.205	121.785
55	45.930	5.642	207.457	181.671	13.859	11.038	65.681	42.716	235.425
56	24.351	1.099	63.715	50.990	5.794	5.244	30.912	18.737	74.971
57	17.377	1.564	68.877	59.437	7.603	6.821	27.909	19.221	85.448
58	32.795	3.640	67.821	49.603	5.630	3.815	26.084	9.686	63.099
59	55.728	7.819	214.740	182.966	13.182	9.273	61.622	33.758	225.997
60	31.509	4.055	78.766	60.987	7.678	5.651	31.367	15.615	82.252
61	43.924	5.251	145.731	121.143	10.663	8.037	48.377	26.415	155.596
62	39.927	4.713	122.918	100.598	10.050	7.694	46.979	27.016	135.307
63	47.344	6.044	155.718	124.324	11.364	8.342	56.187	32.515	164.881
64	18.276	1.816	30.113	20.067	5.194	4.287	19.450	10.312	34.666
65	37.560	5.057	116.256	84.957	8.305	5.777	37.569	18.789	109.523
66	34.158	3.213	118.451	99.765	9.281	7.675	43.899	26.82	134.260
67	30.741	2.878	86.615	70.005	8.055	6.617	35.407	20.037	96.659
68	20.222	1.615	44.091	33.172	5.850	5.042	22.546	12.435	50.650
69	26.922	2.752	60.229	45.392	6.394	5.018	26.206	12.745	63.154
70	28.289	3.066	61.170	45.492	6.678	5.145	27.723	13.579	64.217
71	29.883	1.939	94.016	78.105	7.559	6.590	36.166	21.225	105.920
72	32.468	4.020	86.833	68.588	7.643	5.633	35.273	19.039	93.260
73	40.031	3.324	142.183	120.505	8.855	7.193	46.774	26.758	154.456
74	49.586	5.531	206.684	173.126	10.767	8.001	61.434	36.641	217.768
75	55.728	6.573	197.287	166.637	11.145	8.359	63.674	35.817	210.805
76	47.391	5.332	186.867	160.556	10.664	7.998	61.123	37.428	205.932
77	31.515	5.311	78.492	52.478	7.586	4.931	29.848	14.097	71.100
78	30.767	5.159	66.361	48.398	6.794	4.214	27.835	12.451	65.163
79	24.522	4.796	43.191	28.532	5.604	3.206	18.050	5.789	37.526
80	43.949	7.704	121.111	95.285	9.886	6.034	46.274	24.099	125.419
81	23.776	2.822	48.124	34.825	6.196	4.785	24.261	12.374	51.983
82	18.293	1.168	35.946	26.215	5.228	4.644	18.494	9.347	40.207
83	36.487	4.148	115.217	94.990	8.904	6.830	46.103	27.859	129.589
84	36.637	4.404	92.464	71.947	8.034	5.832	37.709	19.394	97.174
85	35.667	3.086	101.135	81.759	7.638	6.095	38.045	20.211	108.065
86	24.369	.261	59.652	47.337	5.535	5.405	26.687	14.502	67.244
87	12.390	.983	17.517	10.831	3.274	2.782	14.466	8.271	21.884
88	24.563	.177	67.324	54.654	5.931	5.842	32.758	20.477	80.973
89	24.829	2.855	53.949	42.137	6.392	4.964	25.524	13.111	58.180
90	23.987	3.146	49.172	35.636	6.354	4.781	24.777	12.783	53.170
91	63.733	5.464	260.838	226.239	11.412	8.680	73.731	41.864	276.784
92	45.521	5.780	147.232	121.581	10.253	7.363	48.342	25.582	154.526
93	47.421	6.053	144.066	113.329	9.121	6.094	46.967	23.256	142.679
94	53.147	7.433	197.972	167.682	12.978	9.261	61.539	34.966	211.909
95	42.285	5.150	136.471	114.754	10.134	7.559	46.911	25.768	148.081
96	50.488	7.567	132.362	103.335	13.082	9.298	59.655	34.411	147.045
97	41.281	1.259	177.674	156.483	10.920	10.290	57.266	36.626	203.319
98	43.122	6.010	128.233	103.637	9.542	6.537	48.826	27.265	137.440
99	42.395	5.143	139.563	115.794	10.008	7.436	54.564	33.366	156.596
100	32.643	5.043	66.844	48.301	6.553	4.031	26.749	10.428	62.460
MEAN VALUE	37.423	4.167	121.194	100.429	8.779	6.726	43.780	25.069	132.223
AVG VALUE CONTRIBUTION ON TOTAL DOWNWARD FLUX IN PERCENT.....				73.97		5.96		20.07	

Table 2. Selected 62 case atmospheres as indentified from the Wark-catalog, and the computed downward flux from program RADFLUX.

4. Determination of Channel 4 Upward Flux of Radiation.

For each sounding case, the filter-normalized upward flux in the wavelength of 5μ to 30μ was available as a result of computations furnished by Lienesch. This was in the form of the "so-called" channel 4 specific intensity at the top of the atmosphere. Channel 4 specific intensity $I_4(\theta)$ was then transformed to a channel 4 flux for each of the selected 62 cases by using the trapezoidal rule for integration on $I_4(\theta)$ as given by

$$\phi F_4 = 2\pi \int_0^{\frac{\pi}{2}} I_4(\theta) \frac{d(\sin^2\theta)}{2} \tag{17}$$

and its corresponding finite difference form is given by

$$\phi F_4 = 2\pi \left[\sum_{\theta_i=0}^{\pi/2} \frac{I_4(\theta_i)+I_4(\theta_{i+1})}{2} X\tfrac{1}{2}(\sin^2\{\theta_{i+1}\} - \sin^2\{\theta_i\}) \right] \tag{18}$$

where i = 1, 2, 3, ..., 5, and $\theta_1 = 0^o$, $\theta_2 = 20^o$, $\theta_3 = 45^o$, $\theta_4 = 60^o$, $\theta_5 = 78.5^o$, and $\theta_6 = 90^o$. The trapezoidal rule was selected instead of other finite integration schemes because of the unequal zenith-angle intervals of integration. Also the channel 4 upward flux relation is the same as that used by Wark et al. [16] which allows for the usual approximation of azimuthal symmetry.

The zenith angles (θ) of the Nimbus II listings went as far as 78.5^o, hence, the specific intensity for $\Theta = 90^o$ was extrapolated by a Lagrangian form expressed by

$$I(\theta) = \frac{I_1(\theta-\theta_2)(\theta-\theta_3)}{(\theta_1-\theta_2)(\theta_1-\theta_3)} + \frac{I_2(\theta-\theta_1)(\theta-\theta_3)}{(\theta_2-\theta_1)(\theta_2-\theta_3)} + \frac{I_3(\theta-\theta_1)(\theta-\theta_2)}{(\theta_3-\theta_1)(\theta_3-\theta_2)} \tag{19}$$

and which reduces to

$$I(90^o) = I_{78.5^o} + 0.6866I_{45^o} - 1.8649I_{60^o} + 1.1783I_{78.5^o} \tag{20}$$

According to Wark et al. [16], radiation for angles greater than 78.5^{o} contributes only about 4 percent of the total flux and the energy obtained by integrating eq. (17) between $0 = 78.5^{o}$ and $\theta = 90^{o}$ lies well within this 4 percent range.

The black body radiation flux (σT_B^4) at the interface is given directly by the interface temperature (^{o}K), and when $\sigma = 0.56687 \times 10^{-7}$ (watts/m^2 $^{o}K^4$), σT_B^4 is in watts/m^2.

The two satellite air mass properties, ϕF_4 and σT_B^4, are made available for this study by the foregoing procedures, where T_B is taken equivalent to the channel 2 emittance temperature in a simulated Nimbus readout. Moreover, the foregoing integration employing eqs. (18) and (20) were incorporated in the author's computer program SUMFLUX (Appendix I C). The 62 selected Nimbus II cases as well as the computed air mass properties are shown in Table 3.

5. Statistical Results and Inferences

The object in the statistical treatment which follows is to obtain a specification equation for F_d in terms of satellite readouts and other readily accessible air-mass data. To accomplish this, there was available a BMD03R computer program that executes the multiple regression analysis establishing a regression plane given by the linear form of

$$Y = A_o + A_1Z_1 + A_2Z_2 + A_3Z_3 + A_4Z_4 + A_5Z_5 \qquad (21)$$

with the final results of the regression plane shown in Table 4.

The original set of 62 independent data atmospheres was split randomly into two equal sets. One set, Sample A which is denoted by the asterisks in Table 3, was used to develop the regression while the

Table 3. Channel 4 filtered flux and interface black body flux on the 62 case simulated Nimbus II data.

CASE	INTERFACE PRESSURE	INTERFACE TEMPERATURE	CHANNEL 4 FLUX	BLACK BODY FLUX
* 2	1000	289	181.076	395.435
* 3	1009	289	186.376	395.435
* 4	1014	284	171.133	368.771
* 7	998	267	153.014	288.090
* 8	1000	262	143.171	267.109
* 10	1000	298	189.664	447.042
* 12	923	282	170.847	358.492
* 13	1003	278	163.286	338.581
20	850	291	188.125	406.495
23	1000	274	155.662	319.511
27	941	258	140.013	251.167
31	1020	235	105.440	172.884
50	850	275	164.415	324.201
51	850	268	156.219	292.430
52	500	261	144.776	263.054
53	830	275	163.762	324.201
54	703	264	140.085	275.359
55	908	285	184.727	373.993
56	526	249	120.077	217.912
57	1006	226	99.153	147.883
58	400	257	133.449	247.295
59	850	291	181.957	406.495
60	500	261	141.883	263.054
61	700	283	175.614	363.604
62	652	274	162.747	319.511
63	754	283	178.669	363.604
64	400	230	96.914	158.633
65	700	267	143.358	288.090
66	700	266	145.276	283.798
67	568	261	140.226	263.054
68	500	238	106.511	181.883
69	700	248	119.152	214.432
70	700	250	122.381	221.434
71	476	264	146.354	275.359
72	466	265	151.586	279.555
73	700	280	165.731	348.430
74	810	285	176.863	373.993
75	930	289	187.088	395.435
76	932	276	164.492	328.942
* 77	500	256	138.983	243.469
* 78	500	253	131.614	232.255
* 79	400	244	118.779	200.929
* 80	806	268	155.021	292.430
* 81	500	242	114.152	194.422
* 82	400	233	101.118	167.073
* 83	800	264	144.337	275.359
* 84	722	263	143.031	271.210
* 85	700	266	145.922	283.798
* 86	720	248	116.863	214.432
* 87	400	221	79.778	135.224
* 88	818	248	117.937	214.432
* 89	500	246	121.593	207.598
* 90	370	251	130.516	224.998
* 92	700	284	178.260	368.771
* 93	700	283	175.544	363.604
* 94	850	289	183.440	395.435
* 95	700	278	167.003	338.581
* 96	850	285	180.008	373.993
* 97	850	282	174.560	358.492
* 98	724	273	163.219	314.872
* 99	900	271	158.044	305.746
*100	700	255	132.669	239.687

remaining set, Sample B, was used to test the stability of the test data on the check-data which was also derived by the author's computer program RADFLUX.

According to Miller [13] and Martin et al. [11], the regression screening analysis uses a F' critical value both to accept and remove individual variables from the regression. The critical F' value utilizes a "probability level" that is a function of the number "k" of predictors tested and of the Sth selected prediction system. The proposed critical value corresponds to the tabulated F' value at a probability level of $\alpha=\alpha^*/(k-S+1)$ with 1 and N-S-1 degrees of freedom, where N is the sample size to be tested. Since the predictors (k=5) have been pre-selected, the selection choice "S" is equal to 1, hence K-S+1 is equal to 5.

The predictors employed are ϕF_4, σT_B^4, u*, the interface pressure "p", and U* which correspond to Z_1, Z_2, Z_3, Z_4 and Z_5, respectively, in eq. (21). The order of the predictors is a vital consideration in describing the "explained sum of squares by the regression." Channel 4 filtered flux (ϕF_4) is referred to as the thermal channel, for its infrared range is 5μ- 30μ, whereas channel 2 filtered flux, the window channel, has an infrared range of 10-11μ. Channel 2 filtered flux, however, is equivalent to the interface black body flux, σT_B^4, and therefore contains very little atmospheric structural information. Prescribing ϕF_4 ahead of σT_B^4 allows ϕF_4 to assume a larger proportion of the explained variance than σT_B^4.

The most readily adaptable test for the significance of the predictor is the F test based upon an analysis of variance. The F statistic is defined as

$$F = \frac{\text{Mean squares explained by the predictor(s)}}{\text{Mean squares not explained by the predictor(s)}} \quad (22)$$

The F statistics derived from the results of the BMD03R program are shown in Tables 4 and 5. These statistics are used to determine the significant specification on F_d by the multivariate regression and by each of the predictors. Significance in this analysis means that the independent variable and/or variables selected for the F test did not affect the outcome of the regression by mere chance at the specified level of belief. For this analysis, an "α" of 0.01 is chosen resulting in a composite 99% confidence level of belief for the multiple regression.

Also shown in Tables 4 and 5 are the tabulated critical F' values and the "α" critical level for rejection of a possible air-mass variable together with the corresponding "F-value upon entry." Since "α*" is chosen to be 0.01, the "α" critical levels for the 5 predictor regression are 0.002. The "F-values upon entry" are defined by

$$F(1,N-m-1) = \frac{\text{Mean Squares explained by the regression}}{\text{Mean Squares not explained by the regression}} \quad (23)$$

where "N" denotes the number of cases in the sample, "m" is the sequential order of the predictors (m = 1, 2....k), "k" is the number of predictors in the regression, and the number pair (1,N-m-1) denotes the number of degrees of freedom associated with the numerator and the denominator, respectively. For example, the "F-value upon entry" for the first predictor (ϕF_4) in the regression is given by

$$F(1,29) = \frac{(\text{Sum of Squares attributable to the regression})/1}{(\text{Sum of Squares not attributable to the regression})/29} \quad (24)$$

The addition of the next predictor, σT_B^4, requires the definition of a new F-statistic specifically restricted to the testing of σT_B^4, after the contribution of ϕF_4 has been excluded. This new F-statistic follows the same form as given by eqs. (22) and (23) but with one less

degree of freedom in the denominator. The remaining independent variables are examined successively in the same manner with a new F-statistic specifically restricted to the testing of the selected variable after the contribution of the variables already tested have been excluded.

The composite F-statistic for the multiple regression is based upon

$$F(k,N-k-1) = \frac{(\text{Sum of Squares attributable to the regression})/k}{(\text{Sum of Squares not attributable to the regression})/(N-k-1)} \quad (25)$$

Use of eq. (25) with the results from Table 4 gives the F-statistic for the 5 predictor multiple regression as F = 116.03 which is far in excess of a critical F'(5,25) = 3.86 appropriate at a 99% confidence level.

The results of Table 4 show not only that the multivariate regression, but also that each of the single variate predictors are significant with the exception of the last independent variable, U*. The "F-statistic upon entry" for U* is 0.90416 in contrast to the required (tabulated) critical F'-value of 14.0 at 99.8% confidence level of belief. This indicates that U* could only have affected the outcome of the multivariate regression by chance at a very low level of probability. An explanation for the lack of significance by ozone could lie in that the computed amounts of ozone in a column of atmosphere are nearly constant across the 62 case sample resulting in a negligible influence on the regression. Since U* showed so little significance in the regression analysis, another analysis was made with U* excluded. The regression plane for the 4 predictor case is given by the linear expression

$$Y' = A'_o + A'_1 Z_1 + A'_2 Z_2 + A'_3 Z_3 + A'_4 Z_4 \quad (26)$$

Table 4. Analysis of variance for the multiple regression in the five-predictor case. (Sample A)

Variable	Mean	Std. Dev.	Reg. Coeff.	Partial Correl. Coeff.	Sum of Squares Added	F-value upon mth entry	Critical F' value at mth entry
Z_1	149.386	27.893	1.7497	0.3683	127026.92	100.583	10.9
Z_2	292.766	78.606	- 0.4863	-0.2436	12631.01	14.740	11.6
Z_3	0.786	0.929	47.4657	0.7323	7718.57	12.805	12.3
Z_4	743.774	209.606	0.1288	0.7591	9269.31	34.403	13.1
Z_5	0.282	0.025	-121.8864	-0.1868	244.52	0.904	14.0
Y	132.095	73.858					

Other pertinent statistics for the multiple regression

F-value F(5,25)	Critical F-value F'(5,25)	Coeff. of Determination (R_5^2)	Multiple Correl. Coeff. (R_5)	Constant value in Regression
116.031	3.86	0.9587	0.9791	-85.5347

with the final results of the multivariate regression shown in Table 5. The same procedures and testing criteria as before were used resulting in each of the 4 predictors as well as the composite set of predictors showing significant contribution on the regression, thus, the 4 predictor regression was selected as the testing regression plane for the independent data sample. The five variate regression equation is given by

$$F_d = -85.535 + 1.750(\phi F_4) - 0.486(\sigma T_B^4) + 47.466(u^*) + 0.129(p) + -121.866(U^*) \quad (27)$$

and the four variate regression equation is given by

$$F_d = -128.089 + 2.022(\phi F_4) - 0.605(\sigma T_B^4) + 49.897(u^*) + 0.129(p) \quad (28)$$

It is interesting to note that the multiple correlation coefficients shown in Tables 4 and 5 decrease very slightly from 0.9791 in the five variate case to 0.9784 in the four variate case. An explanation for this could lie according to Panofsky et al. [15] and Martin et al. [11] that the longest equation may have actually overfitted the first analysis ascribing some of the variation due to small-scale perturbation to U* by chance.

Finally, the 4 predictor regression was tested using Sample B data by an analysis of variance or of mean squares, that is, a test of variation about the regression plane. Again, significance of the regression plane was tested by the F test as given by equation (24).

Total sum of squares with its components is given by

$$\underset{i=1}{\overset{N}{\Sigma}} (y_i-\bar{y})^2 = \underset{i=1}{\overset{N}{\Sigma}} (y_i-y'_i)^2 + \underset{i=1}{\overset{N}{\Sigma}} (y_i-\bar{y})^2 \quad (29)$$

(A) (B) (C)

where "y'_i" denotes the regression estimates for F_d,"y_i" denotes the

Table 5. Analysis of variance for the multiple regression in the four predictor case. (Sample A)

Variable	Mean	Std. Dev.	Reg. Coeff.	Partial Correl. Coeff.	Sum of Squares Added.	F-value upon mth entry	Critical F' value at mth entry, "α" = 0.0025
Z_1	149.386	27.893	2.0216	0.4291	127026.92	100.583	10.6
Z_2	292.766	78.606	- 0.6051	-0.3085	12631.01	14.740	10.67
Z_3	0.786	0.929	49.8971	0.7575	7718.57	12.805	10.74
Z_4	743.774	209.606	0.1292	0.7547	9269.31	34.403	10.82
Y'	132.095	73.858					

Other pertinent statistics for the multiple regression

F-value $F(4,26)$	Critical F-value $F'_{.01}(4,26)$	Coeff. of Determination (R_4^2)	Multiple Correl. Coeff. (R_4)	Constant Value in Regression
145.3482	4.14	0.9572	0.9784	-128.087

observed F_d values as determined by the computer program RADFLUX, and "N" denotes the total number of cases in the independent data sample. Term (A) gives the total sum of squares; term (B) gives the sum of squares of deviations from the regression plane or the sum of squares not explained by the regression; and, term (C) gives the sum of squares of deviations of the regression estimates from the mean $(\overline{y})$ of the observed values or the sum of squares explained by the regression.

The statistics on the independent data sample are given in Table 6. The required (tabulated) critical F'value $[F'(4,26)]$ is equal to 4.14 at 99% confidence level of belief. One can readily see that the "F" statistic for the independent data F(4,26) = 118.2546, is considerably larger than its corresponding tabulated critical F'value, thus the 4 predictor regression verifies as being significant for determining F_d within 99% confidence level of belief.

Furthermore, the results of the 4 predictor regression on the independent data sample were tested for shrinkage using the relation given by

$$\hat{R}_k^2 = 1 - \frac{\text{(Sum of Squares not explained by the regression)}}{\text{(Total Sum of Squares)}} \qquad (30)$$

where $\hat{R}_k^2$ is the effective coefficient of determination and $\hat{R}_k$ is termed the "effective multiple correlation coefficient." The results are shown in Table 6.

The percent shrinkage between the explained sum of squares of samples A and B is given by $R_4^2 - \hat{R}_4^2$. Here R_4^2 is the coefficient of determination for eq. (28) (Sample A data). Table 6 shows that the regression performed exceptionally well on the independent data sample with only a 5.62% amount of variance shrinkage and with a $\hat{R}_4^2$ and $\hat{R}_4$ of 90.1% and 95.1%, respectively.

Table 6. Analysis of variance on the independent data (Sample B)

Source of Variation	Degrees of Freedom	Sum of Squares	Variance
Explained Variance	4	86065.300	2868.8430
Unexplained Variance	26	9462.072	157.6892
Total Variance	30	95527.372	3026.5322

F-value F(4,26)	Critical F' value F'(4,26)	Coeff. of Determination ($\hat{R}_4^2$)	Multiple Correl. Coeff. ($\hat{R}_4$)	Percent Shrinkage
118.2546	4.14	0.901	0.951	5.62

Table 7. Analysis of variance for the multiple regression in the four predictor case (Sample size 62)

Variable	Mean	Std. Dev.	Reg. Coeff.	Partial Correl. Coeff.	Sum of Squares Added	F value upon mth entry	Critical F' value at mth entry, "α" = 0.0025
Z_1	148.930.	26.936	1.8241	0.3966	193258.78	183.953	10.75
Z_2	290.664	74.913	- 0.3906	-0.2179	14284.10	17.287	10.78
Z_3	0.690	0.795	43.2935	0.7216	21210.10	44.667	10.81
Z_4	733.532	197.471	0.0974	0.7304	14693.16	65.185	10.84
Y'	129.582	64.819					

Other pertinent statistics for the multiple regression

F-value F (4,57)	Critical F'-value F'(4,57) .01	Coeff. of Determination (R_4^2)	Multiple Correl. Coeff.	Constant value in Regression
270.0076	3.68	0.9499	0.9746	-129.847

The foregoing analysis showed that the 4 predictor regression was indeed verified on the independent data sample; but, the process of randomly dividing the original 62 Nimbus II cases in order to realize this verification excluded 31 perfectly good cases from the regression analysis, thus, it was decided to obtain a regression based on the entire 62 Nimbus II cases. One should anticipate a more representative regression than the one previously derived, because the sample size is twice as large as that used in the original analysis. Although the new analysis used the same methods and testing criteria as that used in the 31 case sample, it was, however, confined to the 4 predictor analysis because of the earlier findings in the study. The final regression is given by

$$F_d' = -129.847 + 1.824(\phi F_4) - 0.391(\sigma T_B^4) + 43.293(u^*) + 0.097(p) \quad (31)$$

and its corresponding statistics are given in Table 7. It is interesting to note that the multiple correlation coefficient decreased slightly in going from the 31 case analysis to the 62 case analysis. An explanation for this must lie in that the sample B "explained variance" was slightly smaller than that for sample A.

6. Conclusions

The programmed computational system for downward infrared radiation flux due to the absorbing/emitting properties of water vapor, ozone and carbon dioxide is given in Appendix I A by the author's computer program RADFLUX. This program may be readily used for the determination of F_d. The only necessary inputs are pressure (mb), temperature (^oK), water vapor mixing ratio (g/kg), and ozone mixing ratio (cm NTP per mb) for selected levels in a sounding. Moreover, this program can be easily

modified as shown in Appendix I B in order to determine F_d from any pre-selected level to the top of the atmosphere (0.1 mb). It should be noted that the mean ratio of downward radiation flux due to water vapor (F_{wv}) with and without overlap corrections to the total downward radiation flux (F_d) was 73.97% and 85.6%, respectively.

Furthermore, total and filtered channel 4 upward radiation flux can be determined by using the author's computer program SUMFLUX found in Appendix I C. Also, the interface black body flux or its channel 2 equivalent temperature can be readily determined using this same program.

Finally, the multivariate regression equation developed using Sample A Nimbus II air-mass properties for the determination of F_d had an accuracy of 95.1% on the independent test data, Sample B. This can be seen in the foregoing analyses. The explained standard deviation of the Sample A regression was 95.84%, but the resulting explained standard deviation on the independent sample was 95.1%, giving a loss of accuracy of 2.74%. A partial explanation for the loss of accuracy lies in the process itself of developing a regression on a finite random sample. One should not anticipate a regression determined from a finite sample to perform exactly the same way on another sample of the same population. This is inherent in the randomness of the selection process and of the variations within the population. This effect can be anticipated to be partly minimized by using the largest possible sample. Another partial explanation could lie in the assumption that the regression is linear, but in actuality, F_d might vary non-linearly with one or any combination of its predictors. This would indicate that the true regression is some sort of surface and not a plane,

however, since the shrinkage of the multiple correlation was only 2.74%, the regression plane appears to be a good estimate of the true surface or of physical reality. With the advent of improved satellite sensing systems, the regression equations can be expected to be improved by an analysis similar to the one given in this paper. Furthermore, an improvement on the regression plane may be anticipated, if the satellite data as well as the radiosonde data could be stratified to a common level, namely that of the interface. This, of course, would exclude pressure as a possible air-mass predictor, however, one could reasonably expect this stratification to reduce the scatter about the regression plane. Moreover, since the effect of ozone in a column of atmosphere gives a very nearly constant contribution to F_d and, thus, has very little effect on the regression plane, and since one should expect that the regression based on the largest possible sample to be the most representative to the true regression surface, the best regression for the determination of F_d is, therefore, the 4 predictor regression based upon the 62 case Nimbus sample, eq. (31).

BIBLIOGRAPHY

1. Anderson, T. W. An Introduction to Multivariate Statistical Analysis. John Wiley and Sons, 1960.

2. Best, W. H. and Panofsky, H. A. Some Applications of Statistics To Meteorology. The Pennsylvania State College, 1953.

3. Craig, R. A. The Upper Atmosphere Meteorology and Physics. Academic Press, 1965.

4. Crow, E. L., Davis, F. A. and Maxfield, M. W. Statistics Manual. U. S. Naval Ordnance Test Station, 1955.

5. Elsasser, W. M. and Culbertson, M. F. "Atmospheric Radiation Tables," Meteorological Monographs. v. IV, No. 23, August, 1960.

6. Fleagle, R. G. and Businger, J. A. An Introduction to Atmospheric Physics. Academic Press, 1963.

7. Hanel, R. A., Bandeen, W. R. and Conrath, B. J. "The Infrared Horizon of the Planet Earth," Journal of the Atmospheric Sciences. v. II, March, 1963: 73-86.

8. Haltiner, G. J. and Martin, F. L. Dynamical and Physical Meteorology. Mc Graw-Hill, 1957.

9. Keith, W. H. "A Statistical Model for Determination of Radiative Temperature at 'Black Body' Surfaces, Based upon Specific Window Radiance Values Measures Over a Range of Zenith Angles by Nimbus II Radiometer," Thesis. U. S. Naval Postgraduate School, October, 1966.

10. Martin, F. L. "Computed Overlap Transmissivities of Water Vapor in the 15 band of CO_2." Unpublished manufscript. 1967.

11. Martin, F. L., Borsting, J. R., Steckbeck, F. J. and Manhard, A. H. "Statistical Prediction Methods for North American Anticyclones," Journal of Applied Meteorology. v. II, No. 4, August 1963: 508-516.

12. Martin, F. L. and Palmer, W. C. "Statistical Estimates of Computed Water Vapor Radiative Flux from Clear Skies at an Oceanic Location," Journal of Applied Meteorology. v. III, No. 6, December, 1964: 780-787.

13. Miller, R. G. "Statistical Prediction by Discriminant Analyses," Meteorological Monographs. The American Meteorological Society, v. IV, No. 25, 1962.

14. Palmer, C. H. "Experimental Transmission Functions for the Pure Rotation Band of Water Vapor," Journal of the Optical Society of America. v. L, 1960: 1232-1242.

15. Panofsky, H. A. and Brier, G. W. Some Applications of Statistics to Meteorology. Pennsylvania State University, 1958.

16. Wark, D. Q., Yamamoto, G. and Lienesch, J. "Methods of Estimating Infrared Flux Surfaces Temperature from Meterological Satellites," Journal of the Atmospheric Sciences. v. IX, No. 6, September, 1962.

17. Yamamoto, G. "On a Radiation Chart," Science Report. Tohôku University, Series 5, Geophysics, v. IV, 1952.

APPENDIX I

Significant computer programs developed for this study (Sections A, B, and C).

Appendix I, Section A. Computer Program RADFLUX (FORTRAN 63)

```
-COOP,BOX T, TUPAZ J,S/1S/2S,60,40000.
-FTN,L,E.
      PROGRAM RADFLUX
C     PURPOSE OF THIS STUDY IS TO EXAMINE DOWNWARD FLUX
     0DIMENSION TT(13),U(21),UU(16),UUU(23),WATER(21,13),OZONE(16,13),
     1CO2(23,13),RWATER(21),ROZ(16),RCO2(23),P(40),PMEAN(40),PDIFF(40),
     2T(4 ),Q(40),QMEAN(40),QDIFF(40),CQ(40),CQMEAN(40),CQDIFF(40),
     3SFW(40),SFO(40),SFC(40),CFW(40),CFO(40),CFC(40),FUT(40),GUT(40),
     4DUT(40),FF(1),GG(1),DD(1),COTAUF(21),O3TAUF(40),RCOLAP(1),
     5CO2LAP(21),O3RLAP(40),RO3LAP(1),UC(21),COXMIS(21),TCOLAP(1),
     6TO3LAP(1)
      DIMENSION KASE(40),LEVEL(40)
      DIMENSION Z(40),S(40),V(40),R(40)
     0DIMENSION RH2O(40),RO3(40),RRCO(40),TEMP1(40),TEMP2(40),TEMP3(40),
     1ROPE(13),SOPE(13),TOPE(13),TTW(13),TTO(13),TTC(13),RW(13),RO(13),
     2RC(13),RURF(13),SURF(13),TURF(13)
      DIMENSION MKASE(100),ZCOLAP(100),ZO3LAP(100),ZFWV(100),WFWV(100),
     1ZFO3(100),WFO3(100),ZFCO2(100),WFCO2(100),ZTOTAL(100)
      DIMENSION RATIO1(100),RATIO2(100),RATIO3(100)
      READ(50,60) ((WATER(I,J),J=1,13),I=1,21)
      READ(50,60)((CO2(I,J),J=1,13),I=1,23)
      READ(50,60)((OZONE(I,J),J=1,13),I=1,16)
   60 FORMAT(13F6.3)
      READ(50,61)(U(I),I=1,21)
      READ(50,61)(UUU(I),I=1,23)
      READ(50,61) (UU(I),I=1,16)
   61 FORMAT(12F4.0,3F3.0,F2.0,7F3.0)
      READ(50,59) (RWATER(K),K=1,21)
      READ(50,59)(RCO2(K),K=1,23)
      READ(50,59)(ROZ(K),K=1,16)
   59 FORMAT(12F6.2)
      READ (50,701) (COXMIS(I),I=1,21)
  701 FORMAT(5F15.10)
      READ(50,703) (UC(I),I=1,21)
  703 FORMAT(16F4.2)
      DO 62 I=1,13
```

```
  62 TT(I)=I*10-90
     WRITE(51,100)
 100 FORMAT(1H1)
     WRITE(51,63)(TT(I),I=1,13)
  63 FORMAT (4X,13F8.0)
     WRITE(51,100)
     WRITE(51,64) (U(I),(WATER(I,J),J=1,13),I=1,21)
  64 FORMAT(F5.1,13F8.3)
     WRITE(51,100)
     WRITE(51,64)(UU(I),(OZONE(I,J),J=1,13),I=1,16)
     WRITE(51,100)
     WRITE(51,64)(UUU(I),(CO2(I,J),J=1,13),I=1,23)
     INTER=63
     KUT = 0
     CONST=0.4838
 777 READ (50,1000) KZ
1000 FORMAT(I4)
     READ (50,7000) KOUNT
7000 FORMAT(I4)
  10 READ (50,1) (KASE(I),LEVEL(I),P(I),T(I),Q(I),CQ(I),I=1,KZ)
   1 FORMAT(2I3,F9.1,F5.0,F12.4,F10.3)
     WRITE (51,100)
     WRITE (51,2) (KASE(I),LEVEL(I),P(I),Q(I),CQ(I),I=1,KZ)
  20FORMAT(1X,4HCASE,4X,5HLEVEL,4X,8HPRESSURE,6X,3HH2O,7X,5HOZONE//(1X
    1,I4,I8,F14.4,F12.4,F11.3))
     KT= KZ - 1
     SUMW=0.
     SUMO=0.
     SUMC=0.
     CONST1=0.4342944819
     DO 20 I=1,KT
     PMEAN(I)=(P(I)+P(I+1))/2.
     QMEAN(I) =(Q(I)+Q(I+1))/2.
     CQMEAN(I) = (CQ(I)+CQ(I+1))/2.
     PDIFF(I) = P(I)-P(I+1)
     QDIFF(I) = Q(I)-Q(I+1)
```

```
      CQDIFF(I) = CQ(I)-CQ(I+1)
C     THE PURPOSE OF THES SUB-PROGRAM IS TO CALCULATE THE LOG VALUES FOR
C     THE REDUCED OPTICAL PATHS.
      SUMW=SUMW+QMEAN(I)*PMEAN(I)*PDIFF(I)*(1.00705E-6)
      SUMO=SUMO+CQMEAN(I)*PDIFF(I)*(1.E-5)
      SUMC=SUMC+PMEAN(I)*PDIFF(I)*(2.4469E-4)
      SFW(I)=SUMW
      SFO(I)=SUMO
      SFC(I)=SUMC
      IF (SFW(I)) 56,57,58
   58 CFW(I)=CONST1*LOGF(SFW(I))
   56 CONTINUE
      IF (SFO(I)) 52,53,54
   54 CFO(I)=CONST1*LOGF(SFO(I))
   52 CONTINUE
      IF (SFC(I)) 46,47,48
   48 CFC(I)=CONST1*LOGF(SFC(I))
   46 CONTINUE
      GO TO 20
   57 CFW(I)=19.
      GO TO 56
   53 CFO(I)=19.
      GO TO 52
   47 CFC(I)=19.
   20 CONTINUE
     0WRITE(51,4) (I,T(I),P(I),Q(I),PMEAN(I),PDIFF(I),QMEAN(I),SFW(I),
     1SFO(I),SFC(I),I=1,KT)
    40FORMAT(2H I,4X,1HT,6X,1HP,7X,1HQ,4X,5HPMEAN,3X,5HPDIFF,3X,
     15HQMEAN,6X,3HSFW,6X,3HSFO,6X,3HSFC//(I3,F6.0,F8.1,F7.3,2F8.1,4F9.4
     2))
      WRITE(51,100)
      WRITE(51,9) (I,T(I+1),CFW(I),CFO(I),CFC(I),I=1,KT)
    90FORMAT(3H  I,2X,6HT(I+1),7X,3HCFW,17X,3HCFO,17X,3HCFC//(I5,F5.0,
     13E2 .6))
C     NOTE.....ANY LOG VALUE DENOTED AS 19 INDICATES THAT IT HAS BEEN
C     FORCED OUT OF RANGE OF THE  R  VALUE TABLES BECAUSE OF THE  U  VA-
```

```
C     DUE BEING ZERO.  ALSO, NOTE THAT  U   VALUES CAN NOT BE NEGATIVE
C     DUE TO THE ARITHMETIC AND SEQUENTIAL PROCESSES OF THE PROGRAM.
      WRITE(51,100)
      JUMP=1
      KH=
      KO=
      KC=
C     THE PURPOSE OF THIS SUB-PROGRAM IS TO DETERMINE THE SPECIFIC
C     WATER  R  VALUES FOR EACH LEVEL OF EVERY CASE.
      DO 13 I=KOUNT,KT
      TU = T(I+1) - 273.
      WU=CFW(1)
   36 DO 23 K=1,12
      IF(TU-TT(K)) 23,40,50
   50 IF(TU-TT(K+1)) 40,43,23
   23 CONTINUE
      IF(JUMP)289,189,89
   89 WRITE(51,88) KASE(I),T(I+1),WU
  880FORMAT(1X,8H CASE = I4,4X,8H TUH2O =F5.0,5X,11H LOG UH2O =F6.3,23
     1H ARE OUT OF TABLE RANGE)
  133 IF(JUMP)107,26,13
   40 IT=K
      GO TO 65
   43 IT=K+1
      GO TO 65
  101 DO 39 L=1,20
      IF(WU-U(L))39,70,80
   80 IF (WU-U(L+1)) 70,73,39
   39 CONTINUE
      GO TO 89
   70 IW = L
   74 IF(JUMP)120,110,90
   73 IW = L+1
      GO TO 74
  900CALL FFIN(WU,U(IW),U(IW+1),TU,TT(IT),TT(IT+1),WATER(IW,IT),
     1WATER(IW,IT+1),WATER(IW+1,IT),WATER(IW+1,IT+1),FUT(I))
```

```
      KH=KH+1
      RH2O(KH) = FUT(I)
      TEMP1(KH)=T(I+1)
   13 CONTINUE
      WRITE(51,100)
      JUMP=JUMP-1
      DO 26 I=KOUNT,KT
      TU=T(I+1)-273.
      WU=CFO(I)
      GO TO 36
  189 WRITE(51,188) KASE(I),T(I+1),WU
  188 FORMAT(1X,8H CASE = I4,4X,8H TUO3 = F5.0,5X,10H LOG UO3 =F6.3,23H
     1ARE OUT OF TABLE RANGE)
      GO TO 133
  102 DO 105 L=1,15
      IF(WU-UU(L))105,70,106
  106 IF(WU-UU(L+1))70,73,105
  105 CONTINUE
      GO TO 189
  110 CALL FFOZ(WU,UU(IW),UU(IW+1),TU,TT(IT),TT(IT+1),OZONE(IW,IT),
     1OZONE(IW,IT+1),OZONE(IW+1,IT),OZONE(IW+1,IT+1),GUT(I))
      KO=KO+1
      RO3(KO)=GUT(I)
      TEMP2(KO) = T(I+1)
   26 CONTINUE
      JUMP=JUMP-1
      DO 107 I=KOUNT,KT
      TU=T(I+1)-273.
      WU=CFC(I)
      GO TO 36
  289 WRITE(51,288) KASE(I),T(I+1),WU
  288 FORMAT(1X,8H CASE = I4,4X,8H TUCO2 = F5.0,5X,11H LOG UCO2 =F6.3,23
     1H ARE OUT OF TABLE RANGE)
      GO TO 133
  103 DO 108 L=1,22
      IF(WU-UUU(L)) 108,70,109
```

```
  109 IF(WU-UUU(L+1))70,73,108
  108 CONTINUE
      GO TO 289
 1200CALL FFCO2(WU,UUU(IW),UUU(IW+1),TU,TT(IT),TT(IT+1),CO2(IW,IT),
     1CO2(IW,IT+1),CO2(IW+1,IT),CO2(IW+1,IT+1),DUT(I))
      KC=KC+1
      RRCO(KC)=DUT(I)
      TEMP3(KC) = T(I+1)
  107 CONTINUE
      GO TO 77
   65 IF(JUMP)103,102,101
C     THIS SUB-PROGRAM DETERMINES THE FLUX INTEGRAL FOR WATER VAPOR
C     BETWEEN  -80 TO -273 DEGREES CENTRIGADE.
   77 WU = CFW(KT)
      IND = 3
      DO 150 I=1,20
      IF (WU - U(I)) 150,170,180
  180 IF(WU-U(I+1)) 170,173,150
  150 CONTINUE
  170 IW=I
  174 GO TO (220,210,190)IND
  173 IW=I+1
      GO TO 174
  190 CALL RRWAT(WU,U(IW),U(IW+1),RWATER(IW),RWATER(IW+1),FF)
      WRITE (51,191) FF
  191 FORMAT(1X,6H FF = E17.9)
C    THIS SUBPROGRAM DETERMINES THE FLUX INTEGRAL FOR OZONE BETWEEN
C     -80 TO -273 DEGREES CENTRIGADE.
      IND=IND-1
      WU=CFO(KT)
      DO 160 I=1,15
      IF(WU-UU(I))160,170,181
  181 IF(WU-UU(I+1))170,173,160
  160 CONTINUE
  210 CALL RROZ(WU,UU(IW),UU(IW+1),ROZ(IW),ROZ(IW+1),GG)
      WRITE (51,211) GG
```

```
  211 FORMAT(1X,6H GG = E17.9)
C     THIS SUB-PROGRAM DETERMINES THE FLUX INTEGRAL FOR CO2 BETWEEN
C     -80 TO -273 DEGREES CENTRIGADE.
      IND=IND-1
      WU=CFC(KT)
      DO 200 I=1,22
      IF(WU-UUU(I)) 200,170,182
  182 IF(WU-UUU(I+1)) 170,173,200
  200 CONTINUE
  220 CALL RRCO2(WU,UUU(IW),UUU(IW+1),RCO2(IW),RCO2(IW+1),DD)
      WRITE (51,221) DD
  221 FORMAT(1X,6H DD = E17.9)
C     THIS SUB-PROGRAM INTEGRATES THE INTEGRAL  RDT  BETWEEN T  INITIAL
C     TO  T  FINAL IN DEGREES CENTRIGADE.
      IND=IND-1
      AREA1=0.
      AREA2=0.
      AREA3=0.
      TOTAL=0.
      KHH=KH-1
      DO 400 I=1,KHH
      Y=TEMP1(I) - TEMP1(I+1)
  400 AREA1=AREA1+(RH2O(I)+RH2O(I+1))/2.*Y
      WRITE (51,413) AREA1
  413 FORMAT(1X,10H AREA1  = E17.9)
      KOO=KO-1
      DO 401 I=1,KOO
      Y=TEMP2(I) - TEMP2(I+1)
  401 AREA2=AREA2+(RO3(I)+RO3(I+1))/2.*Y
      WRITE (51,414) AREA2
  414 FORMAT(1X,10H AREA2  = E17.9)
      KCC=KC-1
      DO 402 I=1,KCC
      Y=TEMP3(I) - TEMP3(I+1)
  402 AREA3=AREA3+(RRCO(I)+RRCO(I+1))/2.*Y
      WRITE (51,415) AREA3
```

```
  415 FORMAT(1X,10H AREA3   = E17.9)
C     THIS SUB-PROGRAM INTEGRATES THE INTEGRAL  RDT  BETWEEN  T  FINAL
C     TO  80 DEGREES CENTRIGADE.
      MC=
      MO=
      MW=
      KUMP=1
      WU=CFW(KT)
      DO 900 L=1,13
      DO 903 J=1,20
      IF(WU-U(J)) 903,906,909
  909 IF(WU-U(J+1))906,973,903
  903 CONTINUE
      GO TO 900
  906 IW=J
  974 IF(KUMP) 983,982,981
  973 IW=J+1
      GO TO 974
  981 CALL FFFN(WU,U(IW),U(IW+1),WATER(IW,L),WATER(IW+1,L),ROPE(L))
      MW=MW+1
      TTW(MW) = TT(L)
      RW(MW) = ROPE(L)
  900 CONTINUE
      KUMP=KUMP-1
      WU=CFO(KT)
      DO 915 L=1,13
      DO 918  J=1,15
      IF(WU-UU(J)) 918,906,924
  924 IF(WU-UU(J+1)) 906,973,918
  918 CONTINUE
      GO TO 915
  982 CALL FFFN(WU,UU(IW),UU(IW+1),OZONE(IW,L),OZONE(IW+1,L),SOPE(L))
      MO=MO+1
      TTO(MO)=TT(L)
      RO(MO) = SOPE(L)
  915 CONTINUE
```

```
      KUMP=KUMP-1
      WU=CFC(KT)
      DO 930 L=1,13
      DO 933 J=1,22
      IF(WU-UUU(J)) 933,906,936
  936 IF(WU-UUU(J+1)) 906,973,933
  933 CONTINUE
      GO TO 930
  983 CALL FFFN(WU,UUU(IW),UUU(IW+1),CO2(IW,L),CO2(IW+1,L),TOPE(L))
      MC=MC+1
      TTC(MC) = TT(L)
      RC(MC) = TOPE(L)
  930 CONTINUE
      MUMP=1
      TU=TEMP1(KH) -273.
      KL=KH
      KM=KO
      KN=KC
  830 DO 800 K=1,12
      IF(TU-TT(K)) 800,803,806
  806 IF(TU-TT(K+1)) 803,873,800
  800 CONTINUE
      IF(MUMP) 815,812,809
  809 WRITE(51,818) TU
  818 FORMAT(10H TF H2O = F5.0,3X,22H IS OUT OF TABLE RANGE//)
      KL=KL-1
      TU=TEMP1(KL)-273.
      GO TO 830
  803 IT=K
  874 IF(MUMP) 883,882,881
  873 IT=K+1
      GO TO 874
  881 CALL FORGE1(TU,TTW(IT),RW(IT),RH2O(KL),AREA11)
      ADD1=0.
      IM=IT-1
      DO 824 L=1,IM
```

```
      CALL FORGE2(RW(L),RW(L+1),TTW(L),TTW(L+1),RURF(L))
  824 CONTINUE
      DO 827 L=1,IM
  827 ADD1=ADD1+RURF(L)
C     THIS SUB-PROGRAM DETERMINES THE TOTAL FLUX FOR WATER VAPOR WITH-
C     OUT CO2 AND OZONE OVERLAP CORRECTIONS.
  845 AREA1 = AREA1 + ADD1 + AREA11
      WRITE (51,410) ADD1,AREA11,AREA1
  410 FORMAT(1X,8H ADD1 = E17.9,5X,10H AREA11 = E17.9,5X,14HTOTAL AREA1
     1= E17.9)
      MUMP=MUMP-1
      TU=TEMP2(KO) -273.
      GO TO 830
  812 WRITE(51,833) TU
  833 FORMAT(10H TF  03 = F5.0,3X,22H IS OUT OF TABLE RANGE//)
      KM=KM-1
      TU=TEMP2(KM) -273.
      GO TO 830
  882 CALL FORGE1(TU,TTO(IT),RO(IT),RO3(KM),AREA22)
      ADD2=0.
      IM=IT-1
      DO 836 L=1,IM
      CALL FORGE2(RO(L),RO(L+1),TTO(L),TTO(L+1),SURF(L))
  836 CONTINUE
      DO 839 L=1,IM
  839 ADD2=ADD2+SURF(L)
C     THIS SUB-PROGRAM DETERMINES THE TOTAL FLUX FOR OZONE.
  848 AREA2=AREA2 + ADD2 +AREA22
      WRITE (51,411) ADD2,AREA22,AREA2
  411 FORMAT(1X,8H ADD2 = E17.9,5X,10H AREA22 = E17.9,5X,14HTOTAL AREA2
     1= E17.9)
      MUMP=MUMP-1
      TU=TEMP3(KC) -273.
      GO TO 830
  815 WRITE(51,842) TU
  842 FORMAT(10H TF CO2 = F5.0,3X,22H IS OUT OF TABLE RANGE)
```

```
      KN=KN-1
      TU=TEMP3(KN) -273.
      GO TO 830
  883 CALL FORGE1(TU,TTC(IT),RC(IT),RRCO(KN),AREA33)
      ADD3=0.
      IM=IT-1
      DO 851 L=1,IM
      CALL FORGE2(RC(L),RC(L+1),TTC(L),TTC(L+1),TURF(L))
  851 CONTINUE
      DO 854 L=1,IM
  854 ADD3=ADD3+TURF(L)
C     THIS SUB-PROGRAM DETERMINES THE TOTAL FLUX FOR CARBON DIOXIDE.
  857 AREA3=AREA3+ADD3+AREA33
      WRITE (51,412) ADD3,AREA33,AREA3
  412 FORMAT(1X,8H ADD3 = E17.9,5X,10H AREA33 = E17.9,5X,14HTOTAL AREA3
     1= E17.9)
C     THIS SUB-PROGRAM DETERMINES THE CO2 AND OZONE OVERLAP CORRECTIONS.
      JIP=3
      DO 450 I=1,20
      WU=CFW(KT)
      IF(WU-UC(I)) 450,470,480
  480 IF(WU-UC(I+1)) 470,473,450
  450 CONTINUE
      WRITE(51,451)WU
  451 FORMAT(17H LOG UF TAUCO2 = F9.4,3X,22H IS OUT OF TABLE RANGE//)
      RCOLAP=0.
      GO TO 452
  470 IW=I
  474 GO TO (490,491,492)JIP
  490 CONTINUE
  491 CONTINUE
  473 IW=I + 1
      GO TO 474
 4920 CALL AOVLAP(WU,UC(IW),UC(IW+1),COXMIS(IW),COXMIS(IW+1),COTAUF(KT),
     1ADD3,AREA33,DD,RCOLAP)
  452 JIP=JIP-1
```

```
      DO 886 I=KOUNT,KT
  886 03TAUF(I) = EXPF(-0.1167 * SFW(I))
      RO3LAP=O3TAUF(KT)*(ADD2+AREA22+GG)
      KIP=3
      KV=
      DO 549 J=KOUNT,KT
      WU=CFW(J)
      DO 550 I=1,20
      IF(WU-UC(I)) 550,570,580
  580 IF(WU-UC(I+1)) 570,573,550
  550 CONTINUE
      WRITE(51,453) KASE(J),WU
 4530FORMAT(1X,7H CASE =I4,3X,16H LOG UCO2 TAU = F9.4,22H IS OUT OF TAB
     1LE RANGE)
      GO TO 549
  570 IW = I
  574  GO TO (590,591,592)KIP
  590 CONTINUE
  573 IW=I+1
      GO TO 574
 5920CALL BOVLAP(WU,UC(IW),UC(IW+1),COXMIS(IW),COXMIS(IW+1),
     1COTAUF(J),DUT(J),T(J),T(J+1),CO2LAP(J),DUT(J+1))
      KV=KV+1
      CO2LAP(KV) = CO2LAP(J)
  549 CONTINUE
      KIP = KIP - 1
      TCOLAP = RCOLAP
      DO 449 J=1,KV
  449 TCOLAP = TCOLAP + CO2LAP(J)
      DO 454 J=KOUNT,KT
  591 CALL BBVLAP(O3TAUF(J),GUT(J),GUT(J 1),T(J),T(J+1),O3RLAP(J))
  454 CONTINUE
      TO3LAP = RO3LAP
      DO 569 J=KOUNT,KT
  569 TO3LAP = TO3LAP + O3RLAP(J)
C     THIS SUB-PROGRAM DETERMINES THE TOTAL DOWNWARD FLUX FOR EVERY
```

```
C      SOUNDING.
       CALL ASUMF(AREA1,AREA2,AREA3,FF,GG,DD,TCOLAP,TO3LAP,TOTAL)
       WRITE(51,79)(AREA1,AREA2,AREA3,FF,GG,DD,TCOLAP,TO3LAP,TOTAL)
   790FORMAT(2X,5HAREA1,3X,5HAREA2,3X,5HAREA3,6X,2HFF,7X,2HGG,6X,2HDD,
      15X,6HTCOLAP,2X,6HTO3LAP,2X,10HTOTAL FLUX//(1X,7E17.9))
       FWV = AREA1+FF-TCOLAP/2.-TO3LAP/2.
       FO3 = AREA2+GG-TO3LAP/2.
       FCO2 = AREA3+DD-TCOLAP/2.
C      THE FOLLOWING VALUES HAVE UNITS  CAL/CM SQUARE/DAY
       WRITE (51,201) AREA1,FF,AREA2,GG,AREA3,DD,TCOLAP,TO3LAP,FWV,FO3,
      1FCO2,TOTAL
  2010FORMAT(1X,10H AREA1  = E17.9//1X,1 H FF      = E17.9//1X,10H AREA2
      1 = E17.9//1X,10H GG      = E17.9//1X,10H AREA3  = E17.9//1X,10H DD
      2    = E17.9//1X,10H TCOLAP = E17.9//1X,10H TO3LAP = E17.9//1X,10H
      3FWV    = E17.9//1X,10H FO3    = E17.9//1X,10H FCO2   = E17.9///1X,
      423H TOTAL DOWNWARD FLUX = E17.9)
       XAREA1 = AREA1*CONST
       XFF = FF*CONST
       XAREA2 = AREA2*CONST
       XGG = GG*CONST
       XAREA3 = AREA3*CONST
       XDD = DD*CONST
       XCOLAP = TCOLAP*CONST
       XO3LAP = TO3LAP*CONST
       XFWV = FWV*CONST
       XFO3 = FO3*CONST
       XFCO2 = FCO2*CONST
       XTOTAL = TOTAL*CONST
C      THE FOLLOWING VALUES HAVE UNITS WATTS/METERS SQUARE
       WRITE(51,1011) KASE(KT)
 1011 FORMAT(1X,7HCASE = I4)
       WRITE(51,1001) XAREA1,XFF,XAREA2,XGG,XAREA3,XDD,XCOLAP,XO3LAP,XFWV
      1,XFO3,XFCO2,XTOTAL
 1001 FORMAT(1X,10H NAREA1 = E17.9//1X,1 H NFF     = E17.9//1X,10H NAREA2
      1 = E17.9//1X,10H NGG     = E17.9//1X,10H NAREA3 = E17.9//1X,10H NDD
      2    = E17.9//1X,10H NCOLAP = E17.9//1X,10H NO3LAP = E17.9//1X,10H
```

```
     3NFWV   = E17.9//1X,10H NFO3   = E17.9//1X,10H NFCO2  = E17.9//1X,
     423H TOTAL DOWNWARD FLUX = E17.9///)
      INTER=INTER-1
      KUT = KUT + 1
      MKASE(KUT) = KASE(KT)
      ZCOLAP(KUT) = XCOLAP
      ZO3LAP(KUT) = XO3LAP
      ZFWV(KUT) = XFWV
      ZFO3(KUT) = XFO3
      ZFCO2(KUT) = XFCO2
      ZTOTAL(KUT) = XTOTAL
      WFWV(KUT) = XAREA1 + XFF
      WFO3(KUT) = XAREA2 + XGG
      WFCO2(KUT) = XAREA3 + XDD
      IF (INTER) 888,999,777
  999 WRITE (51,100)
      YKUT = KUT
      ADD1 = 0.0
      ADD2 = 0.0
      ADD3 = 0.0
      AVG11 = 0.0
      AVG22 = 0.0
      AVG33 = 0.0
      AVG44 = 0.0
      AVG55 = 0.0
      AVG66 = 0.0
      AVG77 = 0.0
      AVG88 = 0.0
      AVG99 = 0.0
      DO 8050 I=1,KUT
      AVG11 = AVG11 + ZCOLAP(I)
      AVG22 = AVG22 + ZO3LAP(I)
      AVG33 = AVG33 + ZFWV(I)
      AVG44 = AVG44 + WFWV(I)
      AVG55 = AVG55 + ZFO3(I)
      AVG66 = AVG66 + WFO3(I)
```

```
      AVG77 = AVG77 + ZFCO2(I)
      AVG88 = AVG88 + WFCO2(I)
      AVG99 = AVG99 + ZTOTAL(I)
 8050 CONTINUE
      AVG1 = AVG11/YKUT
      AVG2 = AVG22/YKUT
      AVG3 = AVG33/YKUT
      AVG4 = AVG44/YKUT
      AVG5 = AVG55/YKUT
      AVG6 = AVG66/YKUT
      AVG7 = AVG77/YKUT
      AVG8 = AVG88/YKUT
      AVG9 = AVG99/YKUT
      DO 1111 I=1,KUT
      RATIO1(I) = ZFWV(I)/ZTOTAL(I)
      RATIO2(I) = ZFO3(I)/ZTOTAL(I)
      RATIO3(I) = ZFCO2(I)/ZTOTAL(I)
 1111 CONTINUE
      DO 1112 I=1,KUT
      ADD1 = ADD1 + RATIO1(I)
      ADD2 = ADD2 + RATIO2(I)
      ADD3 = ADD3 + RATIO3(I)
 1112 CONTINUE
      ADD11 = (ADD1/YKUT)*100.
      ADD22 = (ADD2/YKUT)*100.
      ADD33 = (ADD3/YKUT)*100.
      WRITE(51,1022) (MKASE(I),ZCOLAP(I),ZO3LAP(I),WFWV(I),ZFWV(I),
     1WFO3(I),ZFO3(I),WFCO2(I),ZFCO2(I),ZTOTAL(I),I=1,KUT)
 1022 FORMAT(1X,85HCASE  H2O-CO2  H2O-O3  UNCOR-   CORRECT-  UNCOR-   CO
     1RRECT-  UNCOR-   CORRECT-  TOTAL/1X,88H      OVERLAP  OVERLAP  REC
     2TED   ED WV    RECTED     ED O3    RECTED    ED CO2   DOWNWARD/1X,8
     34H                        WV FLUX   FLUX     O3 FLUX   FLUX     CO2
     4 FLUX  FLUX     FLUX/(1X,I4,2F8.3,F10.3,3F9.3,3F10.3))
      WRITE(51,1031) AVG1,AVG2,AVG3,AVG4,AVG5,AVG6,AVG7,AVG8,AVG9
 1031 FORMAT(1X,4HMEAN/1X,5HVALUE,F7.3,F8.3,F10.3,3F9.3,3F10.3)
      WRITE(51,1032) ADD11,ADD22,ADD33
```

```
 1032 FORMAT(1X,31HAVG VALUE CONTRIBUTION ON TOTAL/1X,32H  DOWNWARD FLUX
     1 IN PERCENT.....,F6.2,F18.2,F20.2)
  888 END
C      THIS SUBROUTINE EXECUTES FORWARD AND BACKWARD INTERPOLATION TO OBTAIN THE
C      SPECIFIC ELASSER WATER R  VALUE FOR EVERY REDUCED OPTICAL PATH/TEMPERA-
C      TURE PAIR.
       SUBROUTINE FFIN(U,U1,U2,T,T1,T2,FU1T1,FU1T2,FU2T1,FU2T2,F)
       FFUT1=FU1T1+(FU1T2-FU1T1)*ABSF((T-T1)/(T2-T1))
       FFUT2=FU2T1+(FU2T2-FU1T1)*ABSF((T-T1)/(T2-T1))
       F1=FFUT1+(FFUT2-FFUT1)*ABSF((U-U1)/(U2-U1))
       FFUT3 = FU1T2-(FU1T2-FU1T1)*ABSF((T2-T)/(T2-T1))
       FFUT4=FU2T2-(FU2T2-FU2T1)*ABSF((T2 T)/(T2-T1))
       F2= FFUT3+(FFUT4-FFUT3)*ABSF((U-U1)/(U2-U1))
       F=(F1 + F2)/2.
       END
      0SUBROUTINE FFOZ(U,U1,U2,T,T1,T2,GU1T1,GU1T2,GU2T1,GU2T2,G)
       GGUT1 = GU1T1+(GU1T2-GU1T1)*ABSF((T-T1)/(T2-T1))
       GGUT2 = GU2T1+(GU2T2-GU2T1)*ABSF((T-T1)/(T2-T1))
       G1=GGUT1+(GGUT2-GGUT1)*ABSF((U-U1)/(U2-U1))
       GGUT3=GU1T2-(GU1T2-GU1T1)*ABSF((T2 T)/(T2-T1))
       GGUT4=GU2T2-(GU2T2-GU2T1)*ABSF((T2 T)/(T2-T1))
       G2=GGUT3+(GGUT4-GGUT3)*ABSF((U-U1)/(U2-U1))
       G=(G1+G2)/2.
       END
      0SUBROUTINE FFCO2(U,U1,U2,T,T1,T2,DU1T1,DU1T2,DU2T1,DU2T2,D)
       DDUT1=DU1T1+(DU1T2-DU1T1)*ABSF((T-T1)/(T2-T1))
       DDUT2 = DU2T1 + (DU2T2 - DU2T1) * ABSF((T-T1) / (T2 - T1))
       D1=DDUT1+(DDUT2-DDUT1)*ABSF((U-U1)/(U2-U1))
       DDUT3=DU1T2-(DU1T2-DU1T1)*ABSF((T2 T)/(T2-T1))
       DDUT4= DU2T2-(DU2T2-DU2T1)*ABSF((T2-T)/(T2-T1))
       D2 =DDUT3+(DDUT4-DDUT3)*ABSF((U-U1)/(U2-U1))
       D=(D1+D2)/2.
       END
       SUBROUTINE RROZ(U,U1,U2,ROU1,ROU2,GG)
       GG=ROU1+(ROU2-ROU1)*ABSF((U-U1)/(U2-U1))
       END
```

```
      SUBROUTINE RRWAT(U,U1,U2,RWU1,RWU2,FF)
      FF=RWU1+(RWU2-RWU1)*ABSF((U-U1)/(U2-U1))
      END
      SUBROUTINE RRCO2(U,U1,U2,RCU1,RCU2,DD)
      DD=RCU1+(RCU2-RCU1)*ABSF((U-U1)/(U2-U1))
      END
      SUBROUTINE ASUMF(A,B,C,D,E,F,X,Y,Z)
      Z = A+B+C+D+E+F-X-Y
      END
      SUBROUTINE BOVLAP(U,U1,U2,R1,R2,ZZ,D1,T1,T2,XX,D2)
      ZZ= R1 + (R2-R1)*ABSF((U-U1)/(U2-U1))
      XX=ZZ*(D1+D2)/2.*(T1-T2)
      END
      SUBROUTINE AOVLAP(U,U1,U2,R1,R2,Z,A,B,DD,X)
      Z=R1+(R2-R1)*ABSF((U-U1)/(U2-U1))
      X=Z*(A+B+DD)
      END
      SUBROUTINE BBVLAP(A,R1,R2,T1,T2,Z)
      Z= A* ((R1 + R2)/2. * (T1-T2))
      END
      SUBROUTINE FFFN(U,U1,U2,R1,R2,XX)
      XX=R1+(R2-R1)*ABSF((U-U1)/(U2-U1))
      END
      SUBROUTINE FORGE1(TF,T1,R1,RF,X)
      X=(R1+RF)/2.*(TF-T1)
      END
      SUBROUTINE FORGE2(R1,R2,T1,T2,Y)
      Y=ABSF((R1+R2)/2.*(T2-T1))
      END
         END
         FINIS
-EXECUTE.
```

608

Appendix I B. Modification Instructions to Program RADFLUX (FORTRAN 63)

1. Each sounding is subdivided into levels starting from the interface at level I = 1 to the top of the atmosphere (0.1 mb) at level I = KZ. KZ is the number of the last level in the sounding.

2. The following must be completed in order to determine F_d from any preselected reference level different from the interface level:

   a. Note the count or number of the pre-selected level in the sounding and introduce this number as shown below in the example.

      1. Suppose selected reference level is 7 out of 30 levels in a sounding, hence, punch this number on a data card with the unit digit in column 4. This reference level card is the second data card in each of the case atmospheres. Do this procedure anytime the reference level changes for any case-atmosphere.

3. If a level is added or subtracted in a sounding listing, the number on the first data card of the respective case atmosphere must be changed accordingly. For example:

   a. Suppose that there are 29 levels in a sounding, thus, the first data card in the sounding must read 29; however, suppose that 1 level is added to the sounding, thence, the first data card must be changed to read 30.

   b. One must place the unit digit of the specific number in column 4 of the data card.

4. Finally, the INTER (constant) card must replaced when the number of case atmospheres in the study changes. For example:

   a. Presently there are 63 case atmospheres as data input to program RADFLUX, thus, the INTER card reads "INTER = 63."

b. Suppose the data input changes to 100 case atmospheres; thence, the INTER card must be changed to read "INTER = 100."

5. Program RADFLUX was written for FORTRAN 63, however, this program can be made operational in any FORTRAN computer language provided that minor modifications to the control cards are made. One must check with the respective computer language manuals for further information.

Appendix I, Section C. Computer Program SUMFLUX (FORTRAN 63)

```
-COOP,BOX T, TUPAZ J,S/1S/2S,20,20000.
-FTN,L,E.
      PROGRAM SUMFLUX
C     THE PURPOSE OF THIS PROGRAM IS TO INTEGRATE RADIATION INTENSITY
C     CASE.
C     BETWEEN 0 AND 90 DEGREES TO OBTAIN TOTAL UPWARD FLUX FOR EVERY
     0DIMENSION KASE(7),PRES(7),THETA(7),X(7),X2(7),UH2(7),UO3(7),X4(7),
     1TEMP(7),TOTINT(7),CH4INT(7)
      DIMENSION KOUNT(100),PRESS(100),TEMPER(100),CHFLUX(100),
     1BBFLUX(100)
      INTER = 62
      KUT = 0
      CONST=0.56687E-7
      PI = 3.14159
      RADCON = 0.017453
      KZ = 6
      THETA(6)= 90.0
 7770READ (50,2) KASE(1),PRES(1),THETA(1),X(1),X2(1),UH2(1),UO3(1),X4(1
    1),TEMP(1)
   2 FORMAT(I3,F9.1,F8.0,F10.3,2F7.3,F6.3,F10.3,F7.1)
      KT = KZ-1
     0READ (50,3) (KASE(I),THETA(I),X(I),X2(I),X4(I),I=2,KT)
   3 FORMAT(I3,9X,F8.0,F10.3,F7.3,13X,F10.3)
      SUM1=0.
      SUM2=0.
      DO 100 I=1,KT
      CALL FORD1(X(3),X(4),X(5),X4(3),X4(4),X4(5),X(6),X4(6))
      CALL FORD2(X(I),X(I+1),X4(I),X4(I+1),THETA(I),THETA(I+1),TOTINT(I)
     1,CH4INT(I),RADCON)
      WRITE(51,5) KASE(I),I,TOTINT(I),CH4INT(I)
   5UFORMAT(1X,8H CASE = I5,5X,5H I = I4,5X,10H TOTINT = E17.9,5X,10H C
     1H4INT = E17.9//)
      SUM1=SUM1+TOTINT(I)
      SUM2=SUM2+CH4INT(I)
 100 CONTINUE
      WRITE(51,4) (KASE(1),PRES(1),TEMP(1),(I,THETA(I),X(I),X4(I),I=1,KZ
```

```
   1))
  40FORMAT(1X,8H CASE = I5,5X,12H PRESSURE = F5.0,5X,8H TEMP = F5.0//
    1(1X,5H I = I4,5X,10H THETA1 = F5.1,5X,19H TOTAL INTENSITY = F6.3,
    25X,18H CH 4 INTENSITY = F6.3//))
     FLUX1=SUM1*PI
     FLUX2=SUM2*PI
     WRITE(51,6) KASE(1),FLUX1,FLUX2
   6 FORMAT(1X,8H CASE = I5,5X,9H FLUX1 = E17.9,5X,9H FLUX2 = E17.9///)
     CALL FORD3(CONST,TEMP(1),FLUX3)
     WRITE(51,300) FLUX3
 300 FORMAT(1X,9H FLUX3 = E17.9///)
     PRESLN = LOGF(PRES(1))
     INTER = INTER-1
     KUT = KUT + 1
     KOUNT(KUT) = KASE(1)
     PRESS(KUT) = PRES(1)
     TEMPER(KUT) = TEMP(1)
     CHFLUX(KUT) = FLUX2
     BBFLUX(KUT) = FLUX3
     IF (INTER) 888,999,777
 999 WRITE(51,200)
 200 FORMAT(1H1)
     WRITE(51,400) (KOUNT(I),PRESS(I),TEMPER(I),CHFLUX(I),BBFLUX(I),I=1
    1,KUT)
 400 FORMAT(1X,53HCASE    INTERFACE    INTERFACE     CHANNEL 4        BLACK
    1/1X,52H        PRESSURE    TEMPERATURE      FLUX           BODY/49X,
    24HFLUX//(1X,I4,F8.0,F13.0,F15.3,F14.3))
 888 END
     SUBROUTINE FORD1(A,B,C,D,E,F,G,H)
     G = C+0.6866*A -1.8649*B +1.1783*C
     H = F+0.6866*D -1.8649*E +1.1783*F
     END
     SUBROUTINE FORD2(A,B,C,D,E,F,X,Y,Z)
     X=(A+B)/2.*((SINF(F*Z))**2 - (SINF(E*Z))**2)
     Y = (C+D)/2.*((SINF(F*Z))**2 - (SINF(E*Z))**2)
     END
```

```
      SUBROUTINE FORD3(A,B,C)
      C=A*B**4
      END
         END
         FINIS
-EXECUTE.
```

INITIAL DISTRIBUTION LIST

		No. Copies
1.	LT J. B. Tupaz, USN U. S. Naval Academy Annapolis, Maryland	3
2.	F. L. Martin Environmental Sciences U. S. Naval Postgraduate School Monterey, California 93940	5
3.	Library U. S. Naval Postgraduate School Monterey, California 93940	2
4.	Department of Meteorology & Oceanography U. S. Naval Postgraduate School Monterey, California 93940	3
5.	Defense Documentation Center Cameron Station Alexandria, Virginia 22314	20
6.	Office of the U. S. Naval Weather Service U. S. Naval Station (Washington Navy Yard Annex) Washington, D. C. 20390	1
7.	Chief of Naval Operations OP-09B7 Washington, D. C. 20350	1
8.	Officer in Charge Naval Weather Research Facility U. S. Naval Air Station, Bldg. R-48 Norfolk, Virginia 23511	2
9.	Commanding Officer and Director Navy Electronics Laboratory Attn: Code 2230 San Diego, California 92152	1
10.	Officer in Charge Fleet Numerical Weather Facility U. S. Naval Postgraduate School Monterey, California 93940	1
11.	Director, Naval Research Laboratory Attn: Tech. Services Information Officer Washington, D. C.	1
12.	Geophysics Research Directorate Air Force Cambridge Research Center Cambridge, Massachusetts	1

13. Program Director for Meteorology
National Science Foundation
Washington, D. C. 1

14. Director
Environmental Sciences Services Administration
Washington, D. C. 2

15. Office of Naval Research
Department of the Navy
Washington, D. C. 20360 1

16. U. S. Naval Oceanographic Office
Attn: Division of Oceanography
Washington, D. C. 20390 1

17. Office of Naval Research
Department of the Navy
Attn: Geophysics Branch (Code 416)
Washington, D. C. 20360 1

18. Program Director Oceanography
National Science Foundation
Washington, D. C. 1

19. Director
National Oceanographic Data Center
Washington, D. C. 1

20. Chairman
Department of Meteorology & Oceanography
New York University
University Heights, Bronx
New York, New York 1

21. Director
Scripps Institution of Oceanography
University of California, San Diego
La Jolla, California 1

22. Department of Meteorology & Oceanography
Chairman
University of Hawaii
Honolulu, Hawaii 1

23. Department of Meteorology
University of California
Los Angeles, California 1

24. Department of the Geophysical Sciences
University of Chicago
Chicago, Illinois 1

25. Department of Atmospheric Science
Colorado State University
Fort Collins, Colorado 1

26. Department of Engineering Mechanics
University of Michigan
Ann Arbor, Michigan 1

27. School of Physics
University of Minnesota
Minneapolis, Minnesota 1

28. Department of Meteorology
University of Utah
Salt Lake City, Utah 1

29. National Center for Atmospheric Research
Boulder, Colorado 1

30. Department of Meteorology and Climatology
University of Washington
Seattle, Washington 98105 1

31. Department of Meteorology
University of Wisconsin
Madison, Wisconsin 1

32. Department of Meteorology
Florida State University
Tallahassee, Florida 1

33. Department of Meteorology
Massachusetts Institute of Technology
Cambridge, Massachusetts 02139 1

34. Department of Meteorology
Pennsylvania State University
University Park, Pennsylvania 1

35. University of Oklahoma
Research Institute
Norman, Oklahoma 1

36. Atmospheric Science Branch
Fisheries Research Institute
Oregon State College
Corvallis, Oregon 1

37. The University of Texas
Electrical Engineering Research Laboratory
Engineering Science
Building 631A
University Station
Austin, Texas 78712 1

38. Department of Meteorology
Texas A & M University
College Station, Texas 77843 1

39. Lamont Geological Observatory
Columbia University
Palisades, New York 1

40. Division of Engineering and Applied Physics
Room 206, Pierce Hall
Harvard University
Cambridge, Massachusetts 1

41. Department of Mechanics
The Johns Hopkins University
Baltimore, Maryland 1

42. University of California
E. O. Lawrence Radiation Laboratory
Livermore, California 1

43. Department of Astrophysics and Atmospheric Physics
University of Colorado
Boulder, Colorado 1

44. Bureau of Meteorology
Department of the Interior
Victoria and Drummond Streets
Carlton, Victoria, Australia 1

45. International Antarctic Analysis Centre
468 Lonsdale Street
Melbourne, Victoria, Australia 1

46. Department of Meteorology
Mc Gill University
Montreal, Canada 1

47. Central Analysis Office
Meteorological Branch
Regional Adm. Building
International Airport
Dorval, Quebec, Canada 1

48. Meteorological Office
315 Bloor Street West
Toronto 5, Ontario, Canada 1

49. Institut fur Theoretische Meteonologie
Freie Universitat Berlin
Berlin-Dahlem
Thriel-allee 49
Federal Republic of Germany 1

50. Meteorological Service
44, Upper O'Connell Street
Dublin 1, Ireland 1

51. Department of Meteorology
The Hebrew University
Jerusalem, Isreal 1

52. Geophysical Institute
Tokyo University
Bunkyo-ku
Tokyo, Japan 1

53. Department of Meteorology
Insituto de Geofisica
Universidad Nacional de Mexico
Mexico 20, D. F., Mexico 1

54. New Zealand Meteorological Service
P. O. Box 722
Wellington, G. E. New Zealand 1

55. Institute of Geophysics
University of Bergen
Bergen, Norway 1

56. Department of Meteorology
Imperial College of Science
South Kensington
London S.W. 7, United Kingdom 1

57. Meteorological Office
London R.
Bracknell
Berkshire, United Kingdom 1

58. Commonwealth Scientific and Industrial Research
Organization
314 Albert Street
East Melbourne, C. 2, Victoria 1

59. Director
Pacific Oceanographic Group
Nanaimo, British Columbia
Canada 1

60. Naval War College
Newport, Rhode Island 02844 1

61. Superintendent
Naval Academy
Annapolis, Maryland 21402 3

62. Commander, Air Weather Service
Military Airlift Command
U. S. Air Force
Scott Air Force Base, Illinois 62226 2

63. Planetary Sciences Division
National Aeronautics and Space Agency
Greenbelt, Maryland 2

Security Classification

DOCUMENT CONTROL DATA - R&D

(Security classification of title, body of abstract and indexing annotation must be entered when the overall report is classified)

1. ORIGINATING ACTIVITY (Corporate author)
U. S. NAVAL POSTGRADUATE SCHOOL
Monterey, California 93940

2a. REPORT SECURITY CLASSIFICATION
UNCLASSIFIED

2b. GROUP

3. REPORT TITLE COMPUTATIONS OF DOWNWARD RADIATION FLUX BASED UPON A RANDOM SAMPLE OF RADIOSONDE OBSERVATIONS, AND CORRELATION OF THE RESULTS WITH CORRESPONDING SIMULATED NIMBUS II SATELLITE AIR MASS PROPERTIES

4. DESCRIPTIVE NOTES (Type of report and inclusive dates)
MASTER OF SCIENCE THESIS (METEOROLOGY)

5. AUTHOR(S) (Last name, first name, initial)
TUPAZ, Jesus B.
Lieutenant, U. S. Navy

6. REPORT DATE	7a. TOTAL NO. OF PAGES	7b. NO. OF REFS
	68	17

8a. CONTRACT OR GRANT NO.	9a. ORIGINATOR'S REPORT NUMBER(S)
b. PROJECT NO.	
c.	9b. OTHER REPORT NO(S) (Any other numbers that may be assigned this report)
d.	

10. AVAILABILITY/LIMITATION NOTICES
[redacted] GAPL 9/15/69
This document has been approved for public release and sale; its distribution is unlimited.

11. SUPPLEMENTARY NOTES	12. SPONSORING MILITARY ACTIVITY
	Chief of Naval Operations (OP-09B7) Department of the Navy Washington, D. C. 20360

13. ABSTRACT

Relying heavily on the Elsasser and Culbertson (1960) computational system, computations of terrestrial radiation incident at a black body interface have been programmed for an arbitrary atmospheric sounding. The program has been applied to a random sampling of 62 radiosondes from the "Wark-sounding-catalog."

Since Wark et al. (1966) have kindly made available simulated Nimbus II channel 2 and channel 4 specific intensities for these same atmospheres, a multivariate regression was derived relating downward flux computations to Nimbus II channel 2 and channel 4 readouts as well as to two other gross air parameters: (a) total reduced water vapor depth, and (b) interface pressure. All four independent variables gave high statistical significance, with channel 4 filtered flux accounting for the major portion of the "explained variance" of the dependent variable. Total ozone was also tested but yielded no statistical significance on the regression.

DD FORM 1 JAN 64 1473

Security Classification

14. KEY WORDS	LINK A		LINK B		LINK C	
	ROLE	WT	ROLE	WT	ROLE	WT
Analysis of Variance						
Case Atmosphere						
Channel 1 Filtered Flux						
Coefficient of Determination						
Downward Infrared Radiation Flux						
F-critical Tabulated Value						
F-statistic						
Interface						
Interface Black Body Flux						
Multiple Correlation Coefficient						
Multivariate Linear Regression						
Nimbus II						
Optical Path						
Significant Specification						
Sum of Squares Explained						
Sum of Squares Unexplained						
Work-catalog						